Updated: 05 June 2024

Supporting Information

Nano-enzymatic Hydrogel for Cartilage Repair Effectiveness Based on Ternary Strategy Therapy

Wei Deng[1,3,#], Yue Zhou[4,#], Qinlin Wan[6], Lei Li[2], Hui Deng[5], Yong Yin[3], Qingsong Zhou[3], Qiujiang Li[1] , Duo Cheng[3], Xuefeng Hu[5], Yunbing Wang[2,*] & Ganjun Feng[1,*]

[1]Department of Orthopedics Surgery and Orthopedic Research Institute, West China Hospital, Sichuan University, Chengdu 610041, China

[2]National Engineering Research Center for Biomaterials & College of Biomedical Engineering, Sichuan University, Chengdu, Sichuan, 610065, China

[3]Department of Orthopedics, Pidu District People's Hospital, The Third Affiliated Hospital of Chengdu Medical College, Chengdu, 611730, China

[4]Department of Emergency Medicine, West China Hospital, Sichuan University, Chengdu, 610041, China

[5]West China School of Basic Medical Sciences & Forensic Medicine, Sichuan University, Chengdu, Sichuan, 610041, China

[6]Medical College of Soochow University, Suzhou, 215123, China

[#]These authors contributed equally to this work.

*Corresponding author at. 29 Wangjiang Road, Chengdu, China, 610065

Tel: +86 028 85410537; Fax: +86 028 85410246

E-mail addresses: yunbing.wang@scu.edu.cn(Y. Wang)

*Corresponding author. 17 Gaopeng Avenue, Chengdu, China, 610041

Fax: +86-028-85423438; Tel: +86-028-85422570

E-mail addresses: gjfenghx@163.com(G. Feng)

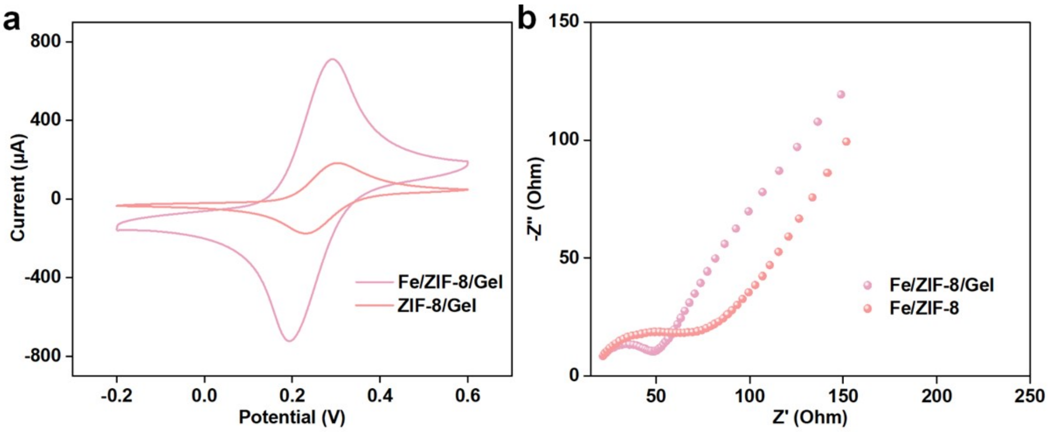

Fig. S1. (a) The CV and (b) the EIS of different types of modified electrodes in 5.0 mM $[Fe(CN)_6]^{3-/4-}$ solution contains 0.1 M KCl.

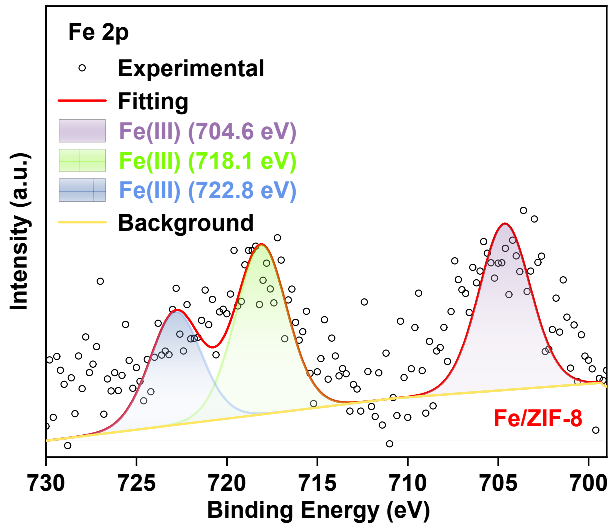

Fig. S2. The high-resolution XPS image of Fe 2p of Fe/ZIF-8.

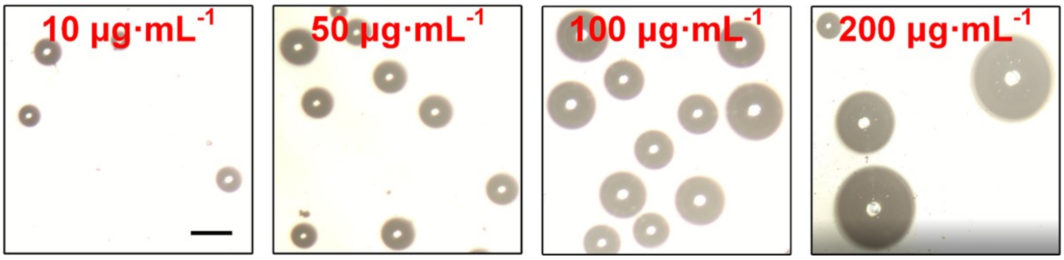

Fig. S3. The optical images of O_2 bubble production were observed when H_2O_2 (25 mM) was catalyzed by different concentrations of Fe/ZIF-8/Gel nano-enzymatic hydrogels for 30 s in acidic PBS (pH 6.5). (Scale bar: 200 μm).

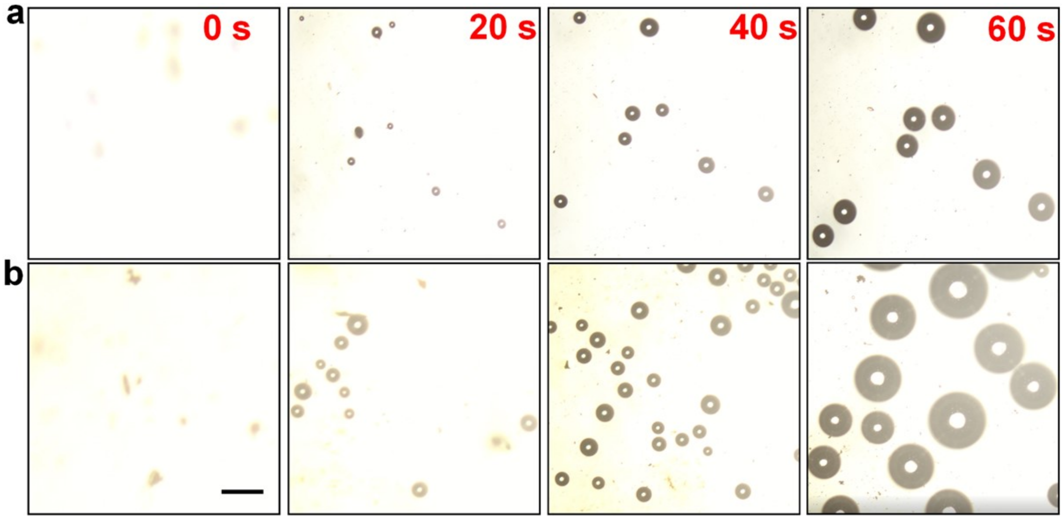

Fig. S4. The O_2 bubbles produced by Fe/ZIF-8/Gel and ZIF-8/Gel nano-enzymatic hydrogels catalyze H_2O_2 (25 mM) as observed by optical microscopy (0.01 M PBS, pH=6.5). (Scale bar: 100 μm).

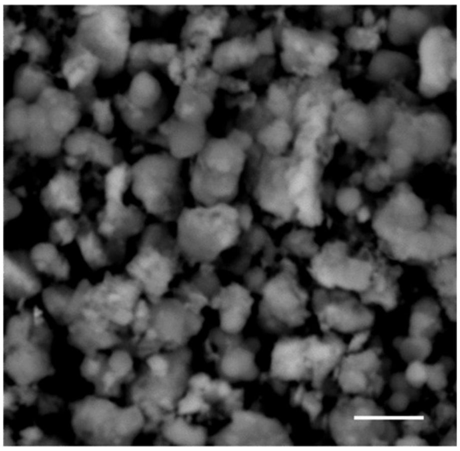

Fig. S5. The SEM image of Fe-MOF. (Scale bar: 2 μm).

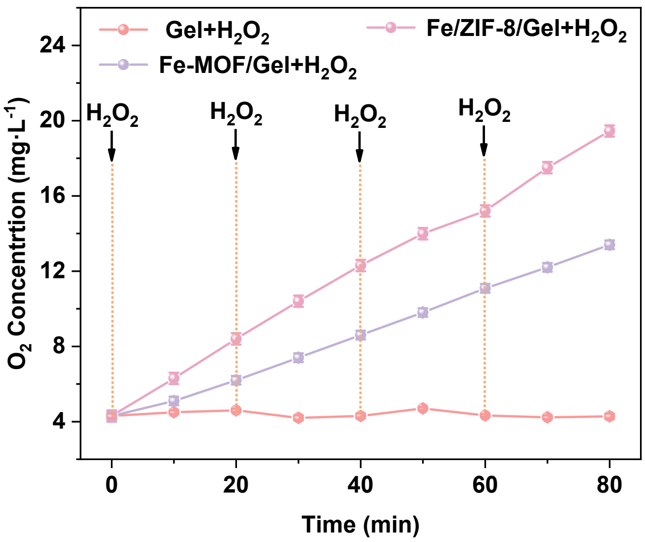

Fig. S6. Continuous catalytic O_2 generation ability of Gel, Fe-MOF/Gel, and Fe/ZIF-8/Gel nano-enzyme hydrogel with a repetitive addition of H_2O_2 (0.1 mM).

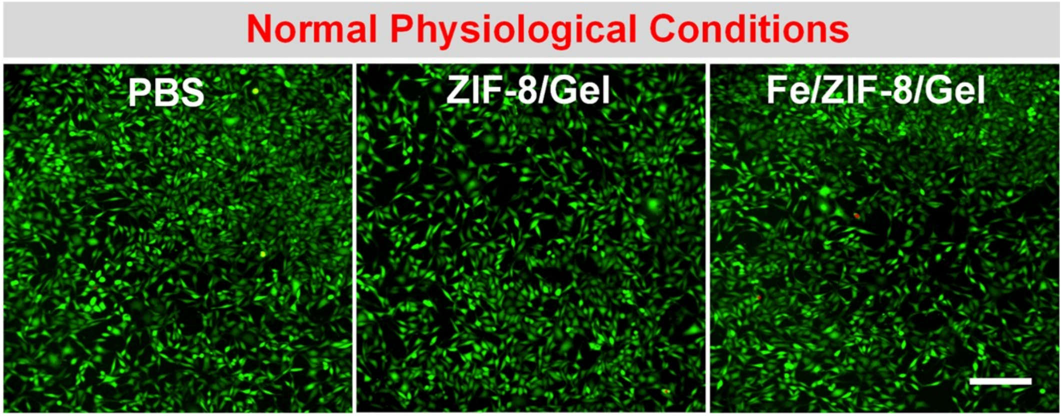

Fig. S7. The Fluorescence images of CHOs stained with Calcein-AM/PI after being treated with PBS, ZIF-8/Gel, and Fe/ZIF-8/Gel. A representative image of three replicates from each group is shown. (Scale bar: 200 μm).

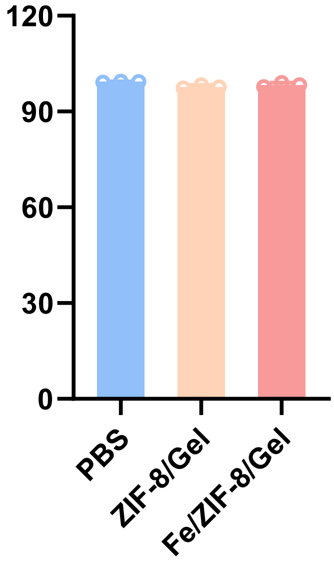

Fig. S8. The quantitative analysis of CHO survival after being treated with ZIF-8/Gel, and Fe/ZIF-8/Gel. Data are presented as mean values ± SD (n = 3).

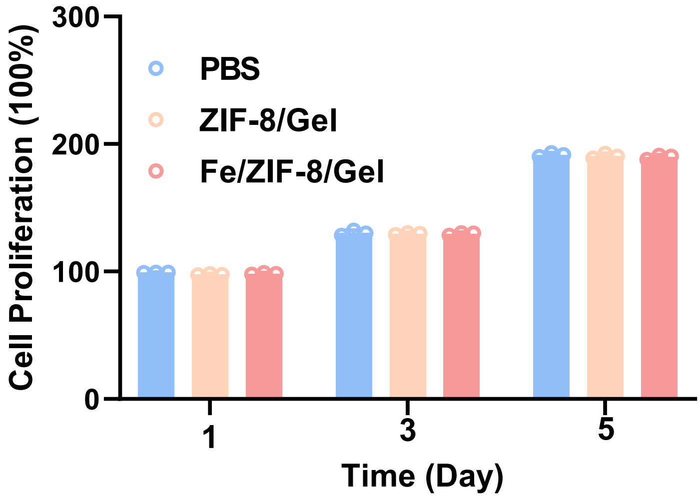

Fig. S9. The quantitative analysis of CHO survival after being treated with ZIF-8/Gel, and Fe/ZIF-8/Gel. Data are presented as mean values ± SD (n = 3).

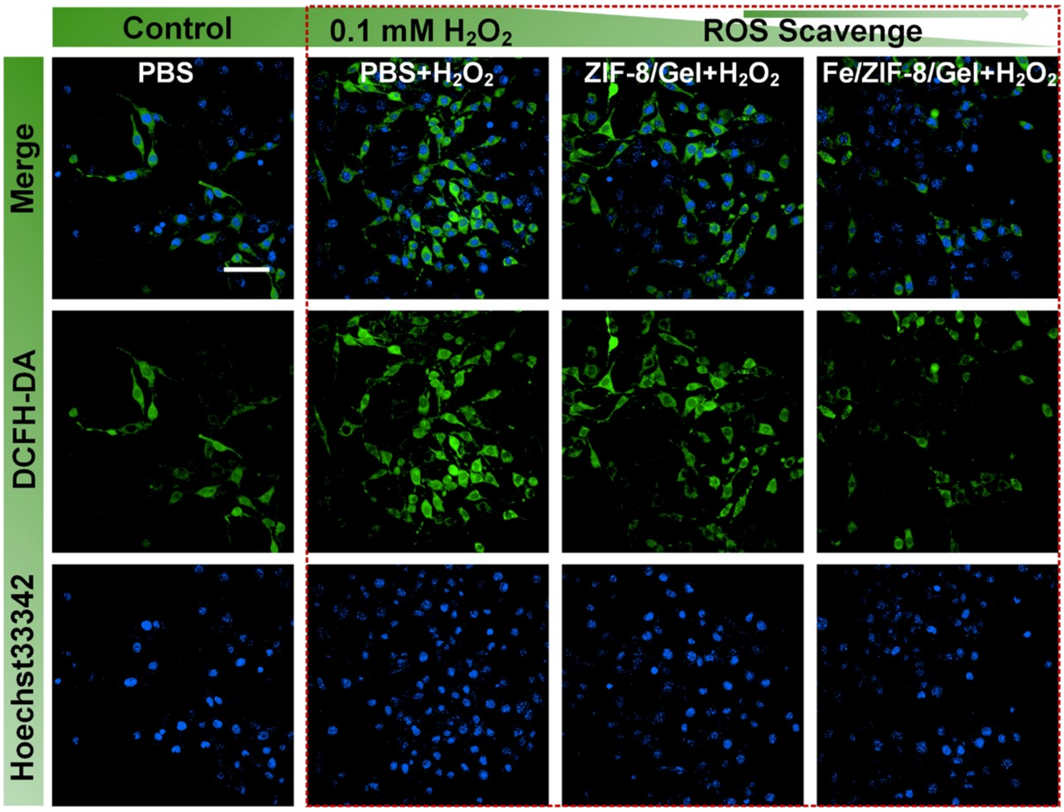

Fig. S10. The ROS scavenge ability was validated by a ROS probe (DCFH-DA) after different treatments. Green fluorescence from DCFH-DA indicates the presence of ROS. (Scale bar: 50 μm).

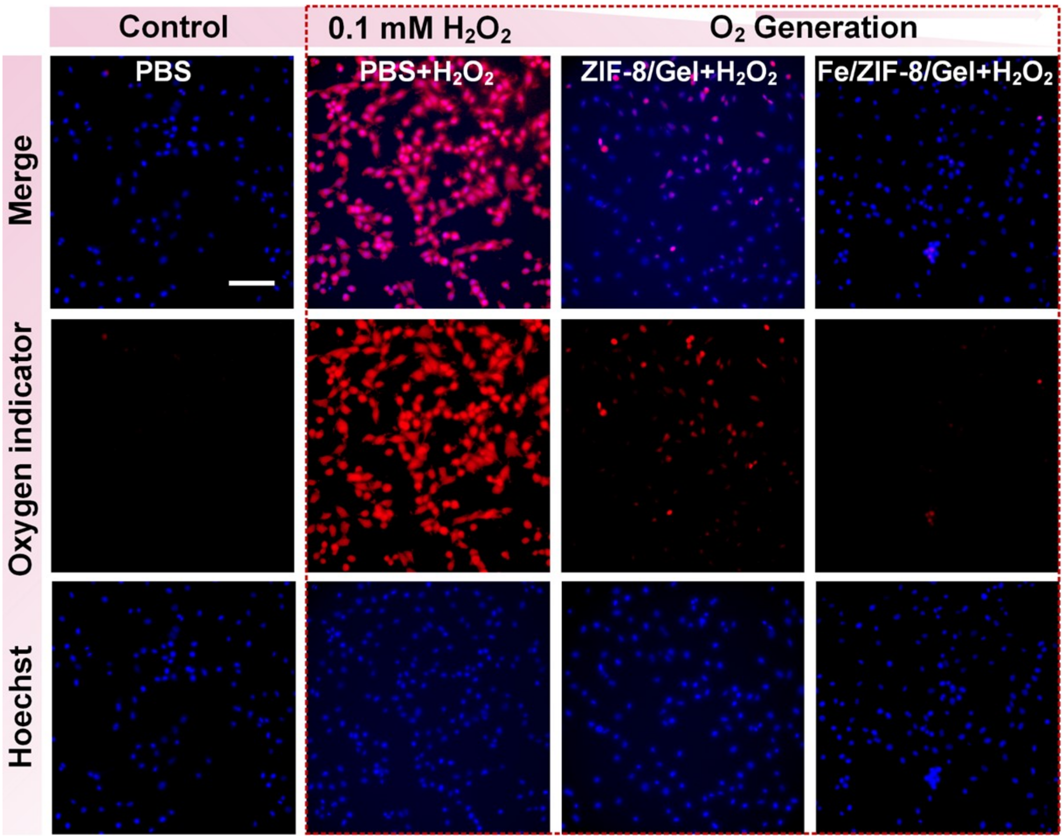

Fig. S11. Intracellular O_2-generation assay monitored by an O_2 probe [Ru(dpp)$_3$Cl$_2$]. Red fluorescence from Ru(dpp)$_3$Cl$_2$ is quenched by O_2. (Scale bar: 100 μm).

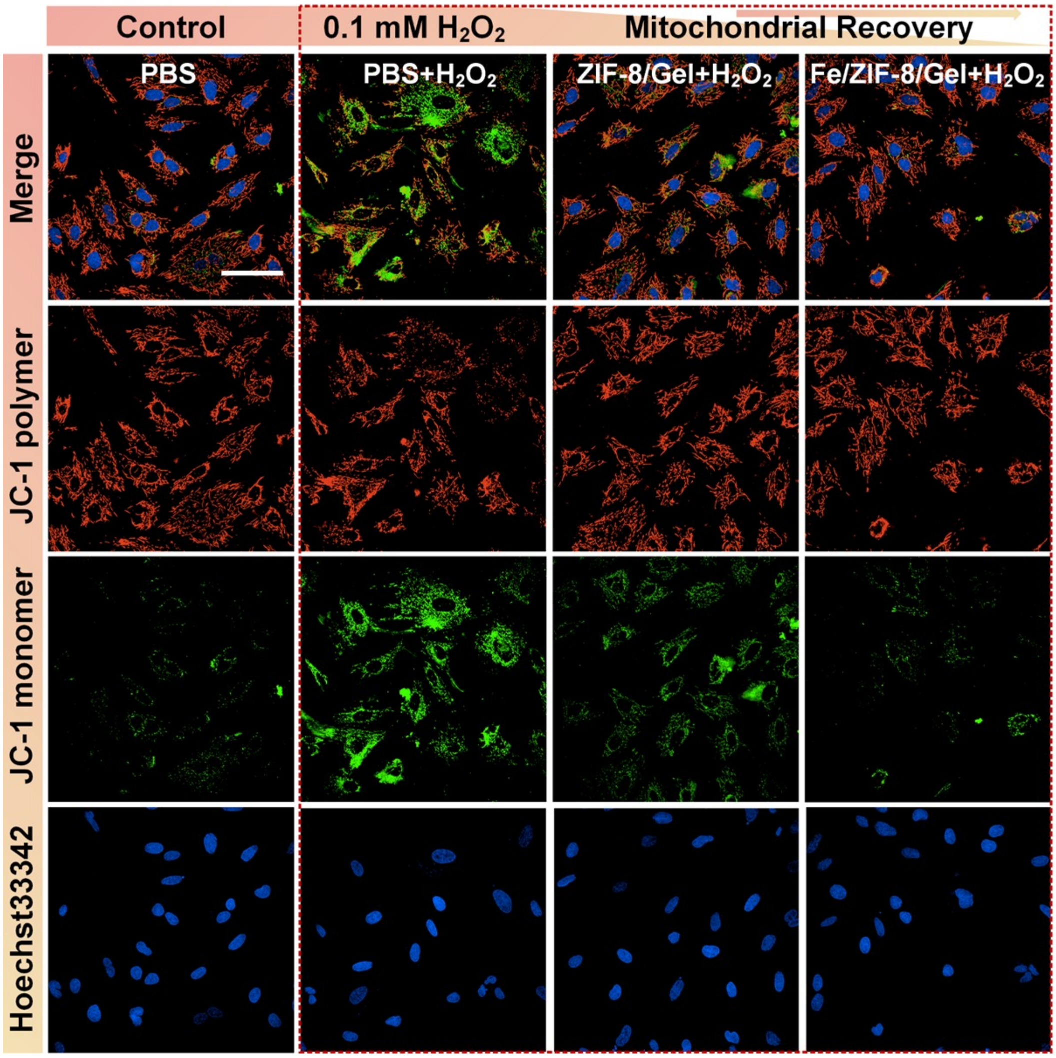

Fig. S12. The JC-1 probe verified mitochondria's membrane potential recovery ability after different treatments. JC-1 emitted green fluorescence to indicate the membrane damage of mitochondria. (Scale bar: 20 μm).

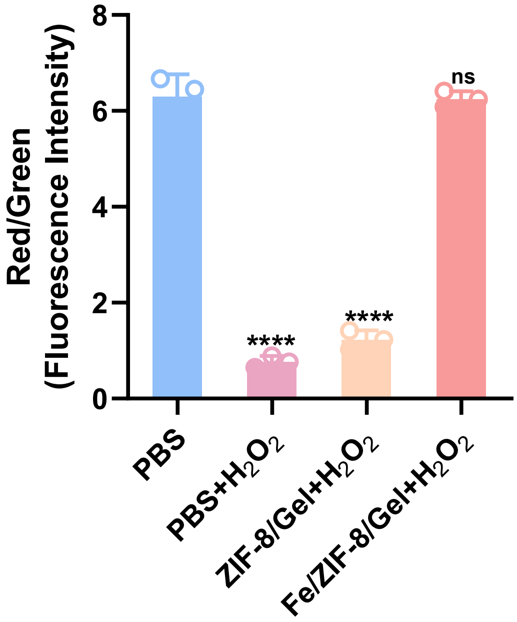

Fig. S13. The quantitative analysis of mitochondrial Δψm in different treatment groups. Data are presented as mean values ± SD (n = 3).

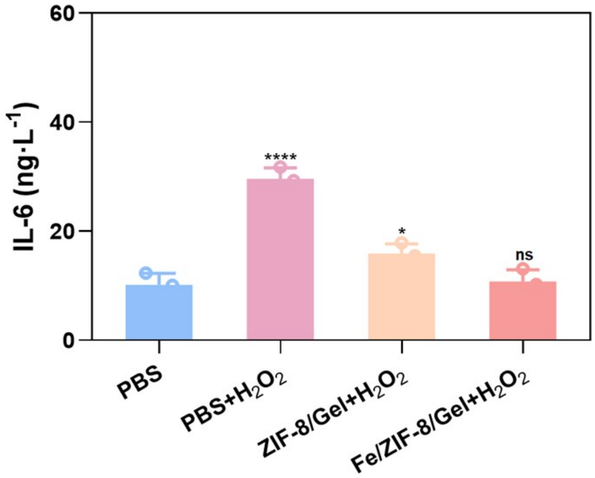

Fig. S14. Expression of IL-6 inflammatory mediators in CHOs after different treatment groups. The Fe/ZIF-8/Gel nano-enzyme hydrogel concentration was 100 μg·mL^{-1} in all experiments. These data are presented as mean values ± SD (n = 3).

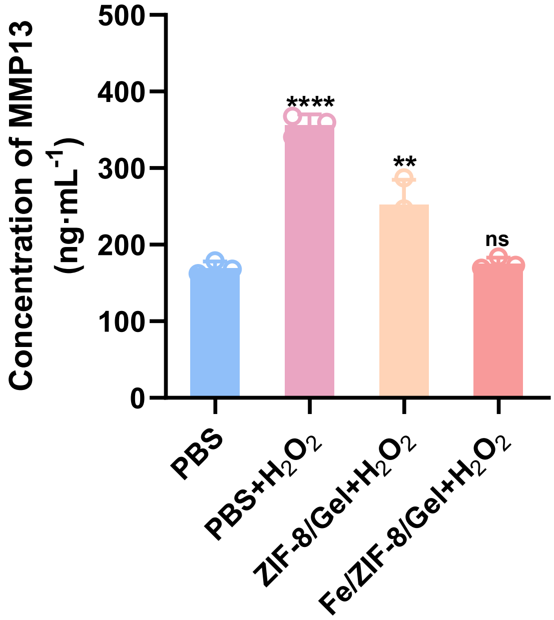

Fig. S15. The quantitative analysis of the inflammatory factor MMP13. Data are presented as mean values ± SD (n = 3).

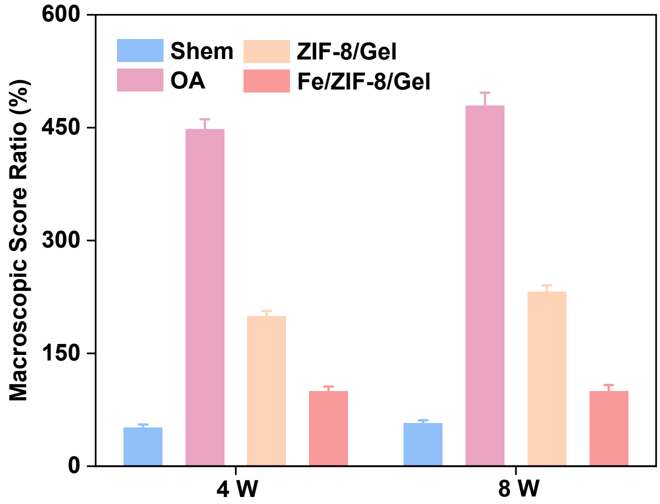

Fig. S16. The Macroscopic score Ratios of knee joints harvested from SD rats after 4 weeks and 8 weeks post-corresponding treatments in different groups. Data are presented as mean values ± SD (n = 3).

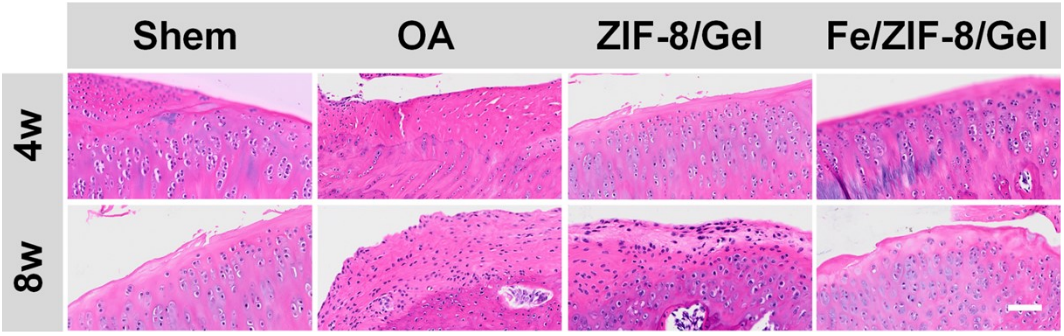

Fig. S17. The optical images of the knee joint stained with H&E after 4 and 8 weeks of treatment in different treatment groups. (Scale bar: 100 μm).

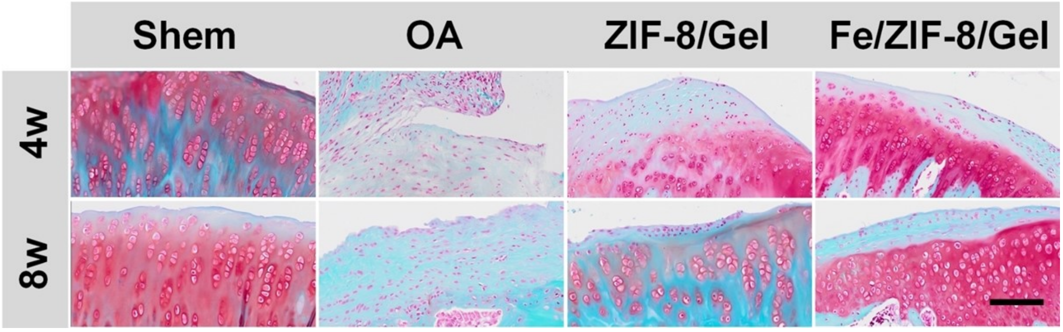

Fig. S18. The optical images of the knee joint stained with safranin O/fast green staining after 4 and 8 weeks of treatment in different treatment groups. (Scale bar: 100 μm).

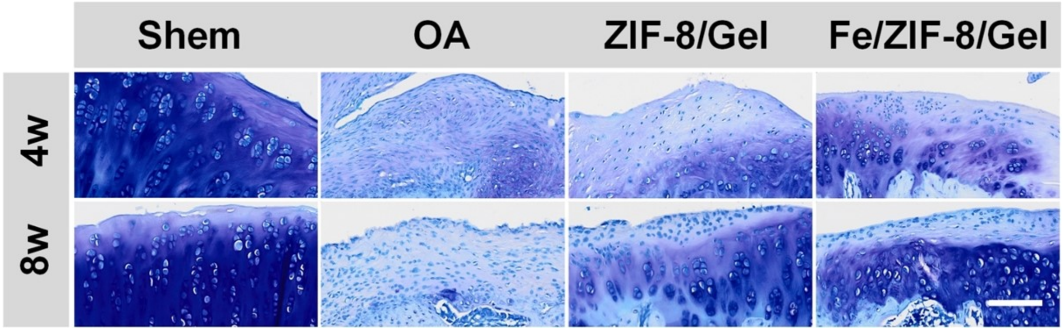

Fig. S19. The optical images of the knee joint stained with toluidine blue staining after 4 and 8 weeks of treatment in different treatment groups. (Scale bar: 100 μm).

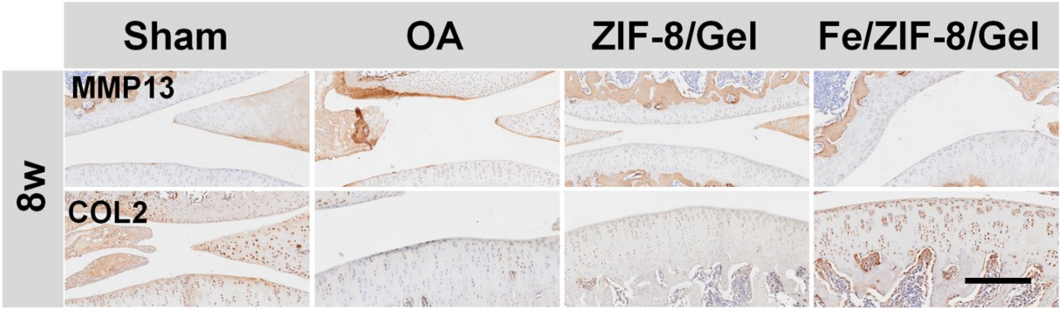

Fig. S20. MMP13 and COL2 sections of joint tissues after 8 weeks of treatment in different treatment groups (Scale bar: 50 μm). (Scale bar: 100 μm).

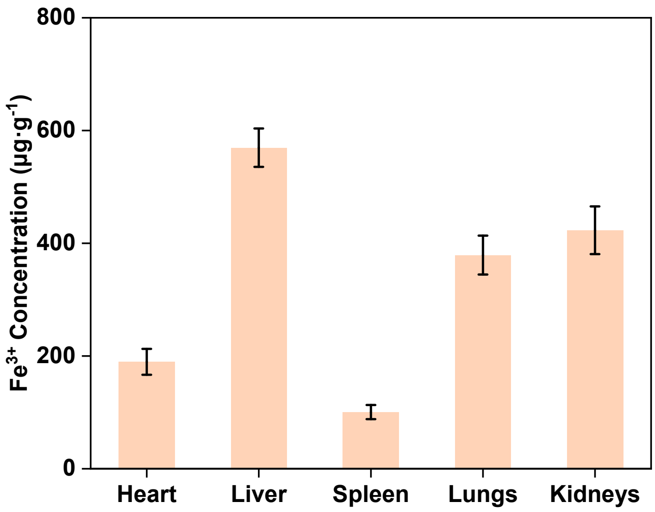

Fig. S21. The iron content in different organs of SD rats after 8 weeks of Fe/ZIF-8/Gel treatment.

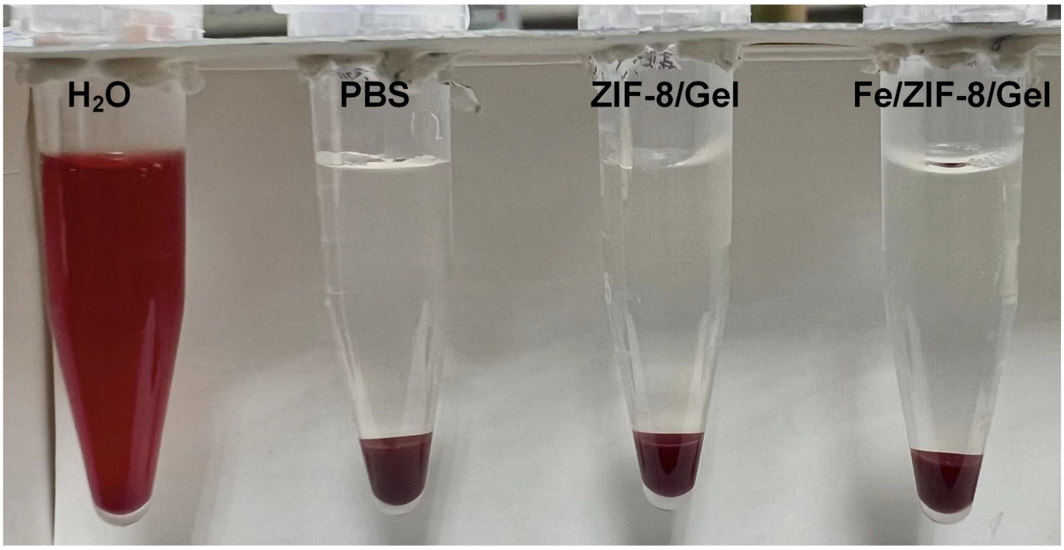

Fig. S22. Hemocyte hemolysis assay after the Fe/ZIF-8/Gel nano-enzymatic hydrogel incubation.

Table S1. Comparison of this work with the recently reported performance of nano-enzymes in catalyzing the decomposition of H_2O_2

Nanoenzymes	Morphology	Substrates	Application	K_m (mM)	V_{max} (M s^{-1})	Refs.
Cu-TCPP-Mn	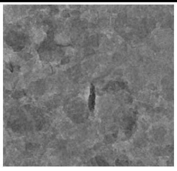 Sheet	H_2O_2	Myocardial injury	34.65	0.357	1
Fh-PVP	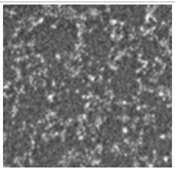 Particle	H_2O_2	Rheumatoid Arthritis	47.24	6.587	2
CuAl-LDH	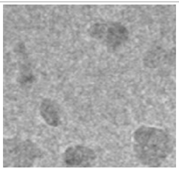 Flake	H_2O_2	Cervical cancer cells	12.08	4.446	3
C-NF	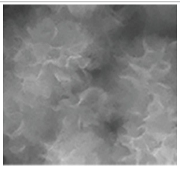 Flower-Like	H_2O_2	Tumor-bearing	0.31	0.0414	4
SAuPTB	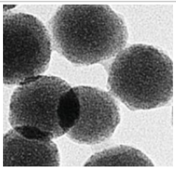 Nanosphere	H_2O_2	Drug-Induced Liver Injury Alleviation	1.50	0.375	5
Mn_3O_4	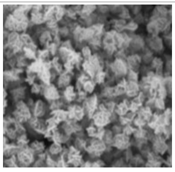 Flower-Like	H_2O_2	Parkinson's disease	0.196	0.933	6
MPMP	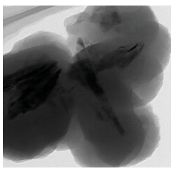 Layered	H_2O_2	OA	10.61	77.92	7

Nanoenzymes	Morphology	Substrates	Application	K_m (mM)	V_{max} ($M\ s^{-1}$)	Refs.
BiPt	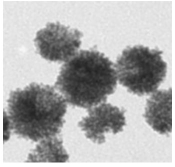 Mesoporous	H_2O_2	Bacterial infection	0.107	7.75	8
Ce-Fe_3O_4	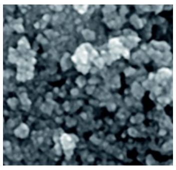 Spherical	H_2O_2	Glucose sensing	0.018	0.0125	9
Mn_3O_4	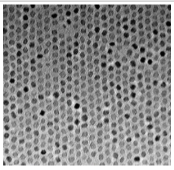 Nanosphere	H_2O_2	OA	0.6	0.583	10
Fe/ZIF-8/Gel	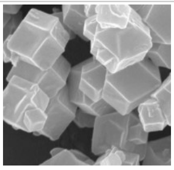 **Dodecahedral**	**H_2O_2**	**OA**	**47.241**	**6.857**	**This work**

C-NF: ZIF-8-derived carbonized nanofibers; SAuPTB: silica-supported ultrasmall gold nanoparticles-tannic acid hybrid nanozyme; MPMP: MoS_2-based nanozyme with stepwise modification of Mg^{2+}-doped polydopamine and zwitterionic polysulfobetaine.

References

1 K. Xiang, H. Wu, Y. Liu, S. Wang, X. Li, B. Yang, Y. Zhang, L. Ma, G. Lu, L. He, Q. Ni and L. Zhang, *Theranostics*, 2023, **13**, 2721-2733.

2 B. Yang and J. Shi, *Nano Lett.*, 2023, **23**, 8355-8362.

3 Z. Wang, J. Liu, M. Feng, K. Song, K. Li, W. Liu, S. Guan and Y. Lin, *Chem. Eng. J.*, 2023, **470**, 144020.

4 Y. Xing, L. Wang, L. Wang, J. Huang, S. Wang, X. Xie, J. Zhu, T. Ding, K. Cai and J. Zhang, *Adv. Funct. Mater.*, 2022, **32**, 2111171.

5 C. Zhou, L. Zhang, Z. Xu, T. Sun, M. Gong, Y. Liu and D. Zhang, *Small*, 2023, **19**, 2206408.

6 N. Singh, M. A. Savanur, S. Srivastava, P. D'Silva and G. Mugesh, *Angew. Chem. Int. Edi.t*, 2017, **56**, 14267-14271.

7 P. Yu, Y. Li, H. Sun, H. Zhang, H. Kang, P. Wang, Q. Xin, C. Ding, J. Xie and J. Li, *Adv. Mater.*, 2023, **35**, 2303299.

8 H. Yao, R. Zhou, J. Wang, Y. Wei, S. Li, Z. Zhang, X. Du, S. Wu and J. Shi, *Adv. Healthc. Mater.*, 2023, **12**, 2300449.

9 M. Hosseini, F. Sadat Sabet, H. Khabbaz, M. Aghazadeh, F. Mizani and M. R. Ganjali, *Anal. Methods*, 2017, **9**, 3519-3524.

10 W. Wang, J. Duan, W. Ma, B. Xia, F. Liu, Y. Kong, B. Li, H. Zhao, L. Wang, K. Li, Y. Li, X. Lu, Z. Feng, Y. Sang, G. Li, H. Xue, J. Qiu and H. Liu, *Adv. Sci.*, 2023, **10**, 2205859.